



Grammatical Fireworks Algorithm Method for Breast Lesion Segmentation in DCE-MR Images

Dipak Kumar Patra, Sukumar Mondal, Prakash Mukherjee

Abstract: For cancer detection and tissue characterization, DCE-MRI segmentation and lesion detection is a critical image analysis task. To segment breast MR images for lesion detection, a hard-clustering technique with Grammatical Fireworks algorithm (GFWA) is proposed in this paper. GFWA is a Swarm Programming (SP) system for automatically generating computer programs in any language. GFWA is used to create the cluster core for clustering the breast MR images in this article. The presence of noise and intensity inhomogeneities in MR images complicates the segmentation process. As a result, the MR images are denoised at the start, and strength inhomogeneities are corrected in the preprocessing stage. The proposed GFWA-based clustering technique is used to segment the preprocessed MR images. Finally, from the segmented images, the lesions are removed. The proposed approach is tested on 5 patients' 25 DCE-MRI slices. The proposed method's experimental findings are compared to those of the Grammatical Swarm (GS)-based clustering technique and the K-means algorithm. The proposed method outperforms other approaches in terms of both quantitative and qualitative results.

Keywords: Breast Cancer, DCE-MRI, Clustering, Warm Programming, Grammatical Fireworks Algorithm.

I. INTRODUCTION

According to the World Health Organization (WHO)'s [38] survey, breast cancer claimed the lives of 6,27,000 people around the world in 2018, accounting for roughly 15% of all cancer deaths among women. Breast cancer is the most common cancer among Indian women, accounting for 14% of all cancers in women [7,15]. In developing countries, organized and opportunistic screening services result in a substantial reduction in breast cancer-related mortality [29].

Dynamic contrast-enhanced magnetic resonance imaging (DCE-MRI) has recently become popular for detecting, diagnosing, and preparing or surgery for breast cancer. Several methods for detecting lesions and characterizing breast DCE-MRI have been developed in the past. Chen et al. [9] used a fuzzy c-means (FCM) clustering method to create an automated breast DCE-MRI segmentation mechanism. FCM is applied to a manually selected enhanced region of interest (ROI) by a human operator. After clustering, the lesion membership map was binarized, and lesions were eventually chosen, with connected-component marking following. A lesion segmentation and classification technique suggested by Nie et al. [26]. First, the Laplacian filter is used to improve the lesions in the ROI that have been manually selected by a human operator. Then, using a Multilayer perceptron, the derived morphology and texture features from lesions were used for classification in benign and malignant lesions (MLP). Yao et al. [40] developed texture features and the discrete wavelet transform (DWT) for breast tumor analysis. The active contour model was used to segment the breast lesions in DCE-MRI for the first time. To obtain the frequency characteristics from the lesion kinematics, texture features were extracted from segmented lesions and DWT was added to the temporal texture features. Finally, the classification was done using a committee of support vector machines (SVM). A Markov Random Field (MRF) model-based lesion segmentation in breast DCE-MRI proposed Wu et al. [39]. The first subtraction image is generated by subtracting the pre-reverse image from the first contrast image in this process, and the ROI is then selected from the subtraction image. The maximum posterior (MAP) of lesion and non-lesion class membership was calculated using the iterative conditional mode (ICM) process. Azmi et al. [3] suggested an improved MRF (IMRF) for lesion segmentation in breast DCE-MRI. The class members' prior distributions are modeled as a ratio of conditional probability distributions of similar and non-similar pixels in a neighborhood. Wei et al. [37] suggested an adaptive moment-preservation approach for segmenting the fibro-glandular tissue of breast DCE-MRI.

Manuscript received on May 22, 2021.

Revised Manuscript received on May 31, 2021.

Manuscript published on May 30, 2021.

* Correspondence Author

D. K. Patra*, Research Centre of Natural and Applied Sciences, Department of Computer Science, Raja Narendralal Khan Women's College (Autonomous), Midnapore (West Bengal), India, E-mail: dpatra11@gmail.com

S. Mondal, Department of Mathematics, Raja Narendralal Khan Women's College (Autonomous) Paschim Medinipur (West Bengal), India, E-mail: sm5971@rediffmail.com

P. Mukherjee, Department of Mathematics, Hijli College Kharagpur (West Bengal), India E-mail: prakashmukherjee25@gmail.com

© The Authors. Published by Blue Eyes Intelligence Engineering and Sciences Publication (BEIESP). This is an [open access](https://creativecommons.org/licenses/by-nc-nd/4.0/) article under the CC BY-NC-ND license (<http://creativecommons.org/licenses/by-nc-nd/4.0/>)



Chang et al. [8] developed a computer-aided diagnosis (CAD) method in DCE-MRI to characterize breast mass lesions of benign and malignant breast tumors. Jayender et al. [18] proposed a statistical learning algorithm to auto-segment the angiogenesis corresponding to a tumor in breast DCE-MRI using Hidden Markov Models (HMMs). Wang et al. [36] developed a hierarchical SVM-based breast DCE-MRI segmentation technique. To classify breast tissues into fatty, fibroglandular, lesion, and skin, 3D multi-parametric features from T1-weighted (T1-w), T2-weighted (T2-w), PD-w, and three-point Dixon water-only and fat-only MRIs were used as inputs to the SVM. In breast DCE-MRI, Milenkovic et al. [23] used logistic regression, vector machine (LS-MV) to help minimum-square-class (LSMD), and minimum-square classification to classify malignant and benign breast lesions. For breast lesion segmentation in DCE-MRI, McClymont et al. [22] used a mean-shift and the graph-cuts algorithm. Wang et al. [14] used modifying FCM for clustering for breast tumor segmentation in DCE-MRI and a pharmacokinetic model to classify additional lesions. Sim et al. [33] proposed a computer-aided detection auto probing (CADAP) method for tumor detection in breast DCE-MRI using a spatial-based discrete Fourier transform, which was further classified as benign, suspect, and malignant. Agner et al. [1] developed the texture kinetics approach for breast lesion categorization in DCE-MR images. On breast DCE-MRI, this approach used a new mark called textural kinetics to distinguish between benign and malignant lesions. Bohare et al. [5] suggested using wavelets to detect cancer in breast MRI images. The input property vector is rendered with presents obtained from the stationary wavelet transform, and the segmentation process is performed by an unsupervised Self-organizing map network. Boukerroui et al. [6] proposed a multiresolution texture-based adaptive clustering approach for breast lesion segmentation. Since the arguments are constructed on manually taken seed points, this texture-based adaptive clustering could be routinely implemented for real-time segmentation in the medical domain. It should be robust to differences in image acquisition settings. Khalvati et al. [19] proposed the Robust Atlas method for automatic breast segmentation in 3D MR images. This approach is based on SWT presentations that looked for MR image categorization, de-noising, compression, and blend, as well as Wavelet.

Cui et al. [11] developed a watershed technique for detecting lesions in DCE-MR images. Dissecting the lesion into 2D slices with the largest region of the lesion is the first step in this process. The Gaussian mixture model is used to measure background markers, marginal lesions, and intensity. The breast model was created by Tuncay et al. [35] using T1-

weighted 3-D MRI data and a realistic microwave. This approach is used to create numerical three-dimensional microwave breast forms with distinct shapes, sizes, and tissue compactness that are as realistic as possible. Hamy et al. [16] developed a robust data decomposition registration method for respiratory motion correction in DCE-MRI. In DCE-MRI, this method is used to decompose into a short rank and a sparse portion. Hauth et al. [17] proposed a three-time-point approach for detecting breast lesions in contrast-enhanced MR mammography. This method transforms the entire breast contrast dynamics information into a color-coded image automatically and reliably. The profile flags method was proposed by Mlejnek et al. [24] for intuitive probing and annotation of volumetric data. As a result, a combination of bend visualization and anatomical data structure terming is developed.

Breast tumor segmentation was developed by Arjmand et al. [2] using K-Means clustering and Cuckoo Search Optimization. They discovered that supervised learning segmentations outperform other methods after testing the methods using the RIDER breast dataset. Three supervised methods have been tested: K-Nearest Neighbors, Bayesian, and SVM. Piantadosi et al. [28] proposed 3TP U-Net, a U-Shaped Deep Convolutional Neural Network with the well-known Three Time Points (3TP) approach that could be used to enhance lesion segmentation. The hard or partitional clustering technique with metaheuristic algorithms is not used in the segmentation of breast DCE-MRI, to the best of the authors' knowledge. This leads to the implementation of a hard-clustering technique with the Grammatical Fireworks algorithm (GFWA) Si et al. [30] in this paper to segment breast MR images for lesion detection. Swarm Programming (SP) is a method for developing automated computer programs in any voluntary language that was created by GFWA. The cluster center for clustering the breast MR images is created using GFWA in this case.

A. Contribution of this article

Now, the contributions in this article is outlined as follows:

- A GFWA-based segmentation methodology is proposed for DCE-MRI to detect breast lesions. A hard-clustering method with GFWA is proposed to segment the breast DCE-MRI.



- GFWA is not used earlier in the segmentation of breast DCE-MRI as well as in any kind of image segmentation. So the application of GFWA in breast lesion detection is another novelty of this article.
- Finally, a comparative study of the proposed technique is conducted with Grammatical Swarm-based clustering technique [31, 32] and K-means algorithm [21].

B. Organization of this article

The rest of this article is organized as follows: The proposed method is given in Section 2. The experimental setup is given in Section 3. The results and discussion are given in Section 4. Finally, a conclusion with the future works is given in Section 5. In the next section, proposed methodology has been discussed.

II. MATERIAL AND METHODS

A. Outline of the Proposed Methodology

The three steps of the devised breast DCE-MRI segmentation method are below:

- Preprocessing
- Segmentation
- Postprocessing

The flowchart of the devised method is specified in Fig. 1 and each steps are expressed in next.

B. Preprocessing

The visual quality of MRI plays a major role in accurately diagnosing the treatment which can be reduced by the existing noise throughout the whole process of acquisition. Both the clinical diagnostic functions and the segmentation process are affected by the noise in MRI [25]. The segmentation process also faces difficulties because of the presence of intensity inhomogeneities (IIHs) in MR images. IIHs are the smooth intensity change inside the originally homogeneous region in the MRI [4]. In this work, the MR images are denoised using Anisotropic Diffusion Filter (ADF) [25], and IIHs are corrected using Max filter-based method [4]. In

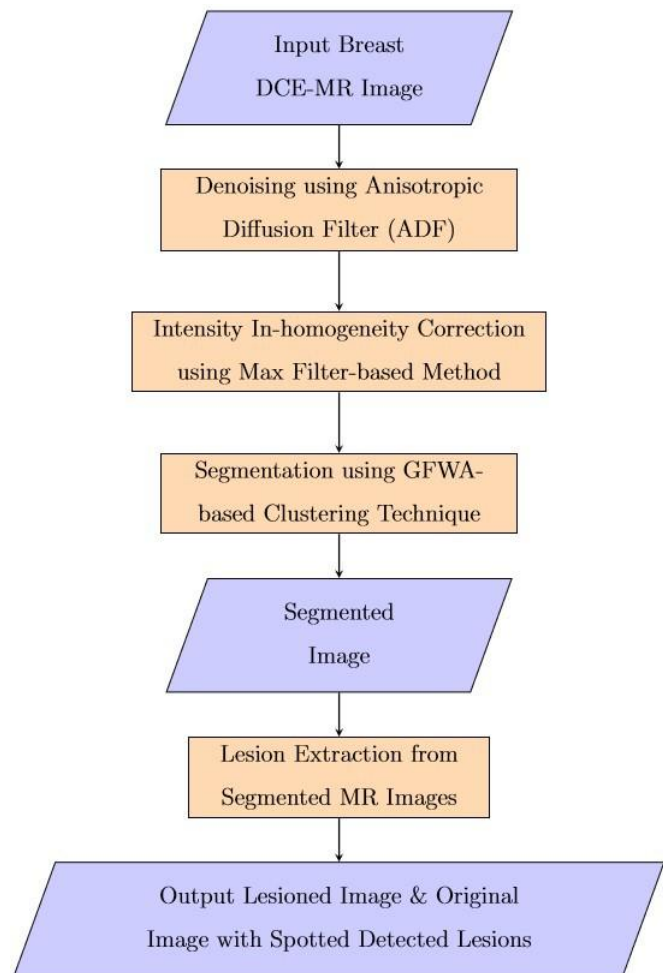


Fig. 1. Outline of the proposed method.

MR images, noise is observed independent of inhomogeneity. The inhomogeneous image (I_h) is modeled as defined by:

$$I_h = I \times B + N \tag{1}$$

where I is homogeneous image, B is inhomogeneity bias field and N is noise. In next, denoising using ADF is discussed.

- Denoising using Anisotropic Diffusion Filter

An ADF is a technique that focuses on removing image noise without changing notable segments of the content of the image. In [27], ADF bears a resemblance to an action that generates a scale area, where an image based on a diffusion process creates a parameterized family of successively more obscure images. Each image obtained as a result of this process is stated as a transition between the image and a 2-D isotropic Gaussian filter, the widths of the filters increase with the parameters.



This evolutionary action is a linear and spatial transmutation of the initial image. ADF is a generalization of this isolated action: it generates a family of parameterized images, but every result image turns on the localized content of the initial image, which is a combination of the initial image and filter image.

let $\Omega \subset R^2$ indicate a subset of the plane and a family of gray scale image indicate $I(., t) : \Omega \rightarrow R$, then ADF is designated as follows

$$\frac{\partial I}{\partial t} = \text{div}(c(u, v, t)\nabla I) = \nabla c \cdot \nabla I + c(u, v, t)\Delta I \quad (2)$$

where Δ indicates the Laplacian, the slope indicated by ∇ , the divergence operator indicated by div and $c(u, v, t)$ indicates the diffusion coefficient. The rate of diffusion denote $c(u, v, t)$, (u, v) denote spatial position, and t is the time parameter of process ordering. This is usually taken as a task of the image slope so that the edges of the image can be saved.

- Max filter-based IHH Correction

After denoising, the image model in Eq. (1) is become as follows:

$$I_h = I \times B \quad (3)$$

The steps of max filter-based IHH correction method [4] are as follows:

1. The max filter is applied to inhomogeneous image (I_h) and the result is considered as bias field:

$$I_b = \text{Max}(I_h) \quad (4)$$

2. Log of the filtered image is subtracted from that of the inhomogeneous image:

$$\log(I_c) = \log(I_h) - \log(I_b) \quad (5)$$

3. The corrected image (I_c) is achieved as follows:

$$I_c = \exp(\log(I_c)) \quad (6)$$

4. Intensity is adjusted to preserve initial dynamics as follows:

$$I_{norm} = \frac{I_c - \min(I_c)}{\max(I_c) - \min(I_c)} \times \max(I_h) \quad (7)$$

C. Segmentation Using GFWA-based Clustering

- Grammatical Fireworks Algorithm

Grammatical Fireworks algorithm (GFWA) [30] is an SP algorithm in which the Fireworks algorithm (FWA) [34] is worked as a learning algorithm in the genotype- to-phenotype mapping process to produce computer programs automatically in any arbitrary

language. In [34], a Swarm Intelligence (SI) algorithm, imitates the explosion procedure of fireworks in the sky at night. There are two types of sparks in the FWA called ‘Explosion Sparks’ and ‘Gaussian Sparks’. The exploitation of local search is carried out by good fireworks by creating a higher number of ‘Explosion sparks’ with lower perturbation whereas exploration or global search is carried out by bad fireworks by creating a lower number of ‘Explosion sparks’ with higher perturbation. ‘Gaussian sparks’ are created by Gaussian mutation in fireworks to create more diversification in the search area. Finally, the crowding distance-based roulette wheel selection is applied to choose the best set of solutions from all types of sparks and original fireworks. The flowchart of FWA is given in Figure 2. The FWA is discussed in next.

Fireworks Algorithm: Fireworks explosion has two specific behavior. When fire- works are good makeup, a number of sparks are created, and the sparks are consolidated the explosion bosom. However, for an inferior firework explosion, hardly any sparks are created and the spark disperses in the area. From a optimization algorithm, firework indicates that the firework situated in a favorable space that perhaps adjacent to the flawless point. It is more suitable to use sparks to explore the local area around the fireworks. A bad firework means that the best position can be very far from the position of the fireworks. Then, Search radius must be large. In the FWA, more sparks are produced and the explosion amplitude is trivial for quality firework, stabilize to a bad one.

The FWA is outlined for the search problem:

$$\text{Minimize } f(u) \in R, \quad u_{\min} \leq u \leq u_{\max}, \quad (8)$$

Where $u = (u_1, u_2, \dots, u_d)$ indicates a position within the potential area, $f(u)$ denotes objective function, u_{\min} and u_{\max} indicate the bounces of the probable area. Next the total unit of sparks created by every firework u_i is designed as beneath:

$$m_i = s \cdot \frac{v_{\max} - f(u_i) + \varepsilon}{\sum_{i=1}^n (v_{\max} - f(u_i)) + \varepsilon} \quad (9)$$

Where s denote parameter managing the total unit of sparks created at the x fireworks, $v_{\max} = \max(f(u_i))$ ($i = 1, 2, \dots, n$) is the maximum value of the impartial function, and ε is the very small constant to avoid “division-by-zero” error.

The bounds are designed for m_i , which is followed by Eq. (10).



$$\hat{m}_i = \begin{cases} \text{round}(x.s), & \text{if } m_i < xs \\ \text{round}(y.s), & \text{if } m_i > ys, x < y < 1 \\ \text{round}(m_i), & \text{otherwise} \end{cases} \quad (10)$$

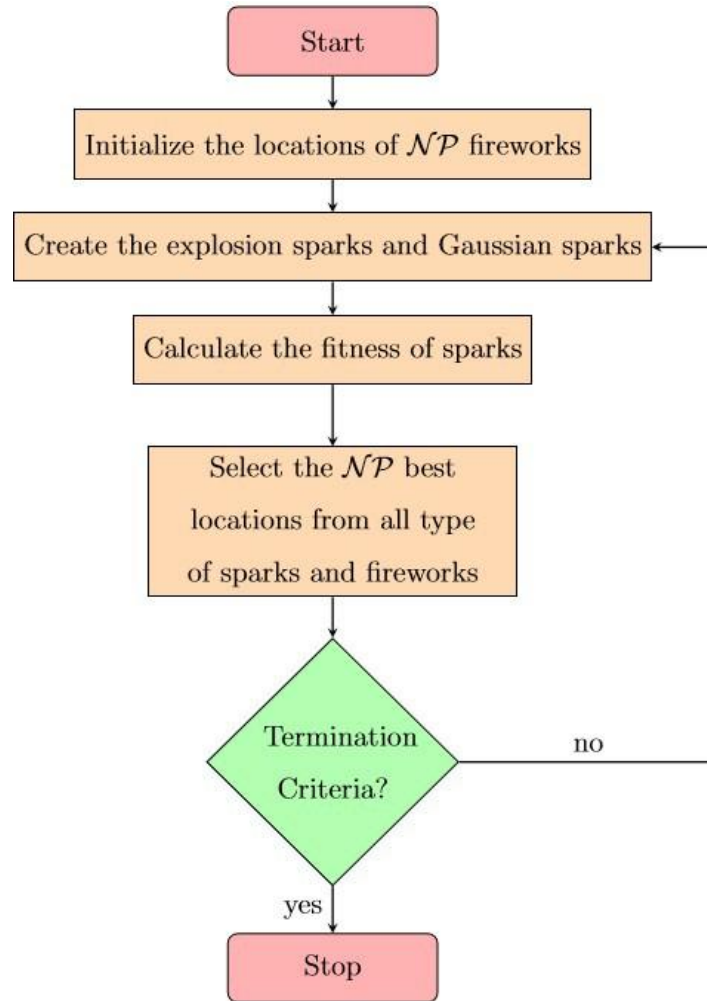


Fig. 2. Flowchart of Fireworks Algorithm.

where x and y are indicating constant parameters. Amplitude value for every firework is calculated as follows:

$$P_i = \hat{P} \cdot \frac{f(u_i) - v_{\max} + \varepsilon}{\sum_{i=1}^n (f(u_i) - v_{\max}) + \varepsilon} \quad (11)$$

where \hat{P} indicates the maximum explosion amplitude, and $v_{\min} = \min(f(u_i))$ is the best value of the impartial function.

In an explosion, the sparks can withstand the consequences of an explosion from a random n direction. It acquires the number of the affected controls haphazardly as below:

$$n = \text{round}(d \cdot \text{rand}(0, 1)) \quad (12)$$

where d denote the depth of the position u , and $\text{rand}(0, 1)$ indicate an uniform dispensation above $[0, 1]$.

Algorithm 1 is calculated as the position of a spark of the firework u_i . The position of spark \tilde{u}_j is first created. If the achieved position is search to disagree with the probable area, it is surveyed to the probable area conforming to the algorithm.

Algorithm 1 The number of sparks and explosion

- 1: Initialize the position of the spark: $\tilde{u}_j = u_i$;
- 2: $n = \text{round}(d.\text{rand}(0, 1))$;
- 3: Haphazardly choose n areas of \tilde{u}_j ;
- 4: Compute the movement: $h = P_i.\text{rand}(-1, 1)$;
- 5: for every dimension $\tilde{u}_k^j \in \{ \text{pre-selected } n \text{ dimensions of } u_j \}$ do
- 6: $\tilde{u}_k^j = \tilde{u}_k^j + h$;
- 7: if $\tilde{u}_k^j < u_k^{\min}$ or $\tilde{u}_k^j > u_k^{\max}$ then
- 8: map \tilde{u}_k^j to the probable area:
 $\tilde{u}_k^j = u_k^{\min} + |\tilde{u}_k^j| \% (u_k^{\max} - u_k^{\min})$;
- 9: end if
- 10: end for

This design is another method of constructing sparks - Gaussian explosion to keep the correlation of sparks, which is recounted in Algorithm 2. A Gaussian (1, 1) function, which specifies a Gaussian distribution with mean 1 and a standard deviation of 1, is employed to explain the coefficient of the explosion.

Algorithm 2 Gaussian sparks

- 1: Initialize the position of the spark: $\tilde{u}_j = u_i$;
- 2: $n = \text{round}(d.\text{rand}(0, 1))$;
- 3: Haphazardly choose z areas of \tilde{u}_j ;
- 4: Compute the coefficient of Gaussian sparks:
 $g = \text{Gaussian}(1, 1)$;
- 5: for every dimension $\tilde{u}_k^j \in \{ \text{pre-selected } n \text{ dimensions of } u_j \}$ do
- 6: $\tilde{u}_k^j = \tilde{u}_k^j . g$;
- 7: if $\tilde{u}_k^j < u_k^{\min}$ or $\tilde{u}_k^j > u_k^{\max}$ then
- 8: map \tilde{u}_k^j to the probable area:
 $\tilde{u}_k^j = u_k^{\min} + |\tilde{u}_k^j| \% (u_k^{\max} - u_k^{\min})$;
- 9: end if
- 10: end for

The z positions should be chosen for the fireworks explosion at the beginning of each explosion creation. In the FWA, the contemporary best position u^* , with the impartial function $f(u^*)$ is optimal amid present

positions, is every time remained for the upcoming explosion generation. Next, $(z - 1)$ positions are chosen based on the distances of other positions to accommodate the variation of the spark. The common distance between a position u_i and other position are described beneath:

$$P(u_i) = \sum_{j=1}^K d(u_i, u_j) = \sum_{j=1}^K \|u_i - u_j\| \quad (13)$$

where K denotes the all current positions of both sparks and also fireworks.

Then the selection possibility of a position u_i is described beneath:

$$r(u_i) = \frac{P(u_i)}{\sum_{j \in K} P(u_j)} \quad (14)$$

Manhattan distance, Euclidean distance, and Angle-based distance are used for distance measurement.

The FWA framework is summarized within the Algorithm 3. Through every explosion creation. Two kinds of sparks are produced as stated by Algorithm 1 & Algorithm 2. In first, the number of sparks with different explosion amplitudes turns on the quality of the corresponding firework ($f(u_i)$). The second algorithm is fabricated applying a Gaussian explosion, which actions search in particular Gaussian space about a firework. After getting the positions, z positions are chosen for the next explosion generation. In the FWA, estimated $z + s + \hat{s}$ function assessments are done in every step. Where s is an argument managing the entire unit of sparks fabricated at the z firework and \hat{s} sparks of this type are fabricated in every explosion generation. The best of a function may be searched in D generations.

Algorithm 3 FWA

- 1: Haphazardly select z positions for fireworks;
- 2: **while** finish test = false **do**
- 3: Set out z fireworks accordingly at the z positions;
- 4: **for** every firework u_i **do**
- 5: The total sparks that the firework yields is computed: \hat{m}_i , according to Eq. 10;
- 6: Obtain positions of \hat{m}_i sparks of the firework u_i apply in Algorithm 1;
- 7: **end for**
- 8: **for** $k = 1 : \hat{s}$ **do**



9: Haphazardly choose a firework u_j ;
 10: Produce a particular spark for the firework apply in Algorithm 2;
 11: **end for**
 12: Choose the top position and remain it for succeeding explosion production;
 13: Haphazardly choose $(z-1)$ positions from the two kinds of sparks and the present reworks as stated by the possibility stated in Eq. (14); 14: **end while**

• GFWA-based Clustering

Grammatical Swarm (GS) based clustering (CGS) technique was first developed for lesion detection in brain MRI [31]. In this work, the GFWA-based Clustering (CGFWA) technique is proposed to segment the breast DCE-MR images in order to detect the lesions. Generally, GFWA is applied to generate computer programs automatically in any arbitrary language. But here, GFWA is used to cluster the breast MR images. The clustering solutions, i.e., cluster centers are calculated using the Backus-Naur Form (BNF) of problem specific predefined Context-Free Grammar (CFG) from the firework's location which is comprised of integer codons in the range [0, 255]. Here, the integer values in the range of possible clustering solutions are [0, 255] because the range of the MR image has gray values [0, 255].

The integer values in [0, 255] are generated using the following grammar [31]:

```

<value>:= <digit1><digit2><digit3> (0)
          2<digit2><digit2> (1)
<digit1>:= 0 (0) | 1 (1)
<digit2>:= 0 (0) | 1 (1) | 2 (2) | 3 (3)
          | 4 (4) | 5 (5)
<digit3>:= 0 (0) | 1 (1) | 2 (2) | 3 (3)
          | 4 (4) | 5 (5) | 6 (6) | 7 (7)
          | 8 (8) | 9 (9)
    
```

For the above BNF, the summary of the number of choices associated with each production rule is specified in Table 1.

To generate one integer value, i.e., cluster center, only four codons in the genotype are needed. If K is the number of clusters, then the dimension of the locations of fireworks in GFWA is $D = 4 \times K$. Figure 3 depicts the genotype-to-phenotype mapping where genotype is the set of integer codons and phenotype is the cluster center. The derivation of cluster center from the codons are given in Figure 4.

Table 1 Number of choices associated with each production rule

Rule No.	Choices
1	2
2	2
3	6
4	10

The interested readers can also obtain the details of genotype-to-phenotype mapping process from the studies [31, 30, 32–34].

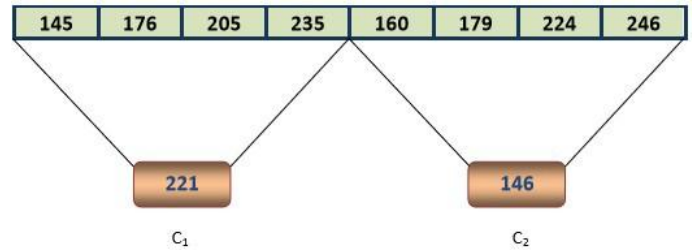


Fig. 3. A genotype (location of fireworks) to phenotype (centroids) mapping

Objective Function Davis–Bouldin (*DB*) index [12] is a familiar and widely used cluster validity index to compute the clustering performance. *DB-index* measure is the ratio of the sum of within-cluster compactness to between-cluster partition. *within ith cluster compactness* is computed as follows:

$$S_{i,p} = \left[\frac{1}{N_i} \sum_{X \in C_i} \|X^p - m_i^p\|^p \right]^{\frac{1}{p}} \quad (15)$$

The inter-cluster distance between i th and j th cluster is computed as:

$$dist_{i,j,p} = \left[\sum_{l=1}^d |m_{i,l} - m_{j,l}|^q \right]^{\frac{1}{q}} = \|m_i^p - m_j^p\|^q \quad (16)$$

where m_i is the center of i th cluster, $p, q \geq 1, p, q$ are integers and N_i is the number of elements in the i th cluster C_i . $R_{i,qt}$ is computed as defined by the following equation:

$$R_{i,qt} = \max_{j \in k, j \neq i} \left\{ \frac{S_{i,p} + S_{j,p}}{dist_{i,j,p}} \right\} \quad (17)$$

Finally, *DB-index* is calculated as follows:

$$DB(K) = \frac{1}{k} \sum_{i=1}^k R_{i,pq} \quad (18)$$

The smallest $DB(K)$ value denotes valid optimal clustering. In the current work, *DB-index* is applied as objective function, i.e., fitness function for fireworks.

D. Postprocessing

In the post-processing step, the lesions are finally extracted from the segmentedMR images using CGFWA method. The cluster centers are sorted in ascending order and pixels are labeled with cluster numbers.



As the pixels belong to the lesion region have the highest labels because the lesioned pixels in DCE-MRI have hyper-intensities, the highest labels are selected to generate the lesioned image. Finally, the lesions are overlaid with the original MR images using the pixel's position of the detected lesions. In the next section, experimental setup is given to conduct the experiments.

III. EXPERIMENTAL SETUP

A. DCE-MRI Dataset

Total 25 Sagittal T2-Weighted DCE-MRI slices of 5 patients have been taken from Cancer Genome Atlas Breast Invasive Carcinoma (TCGA-BRCA) [20, 10]. All MRI slices having size greater than 256×256 are resized to 256×256 .

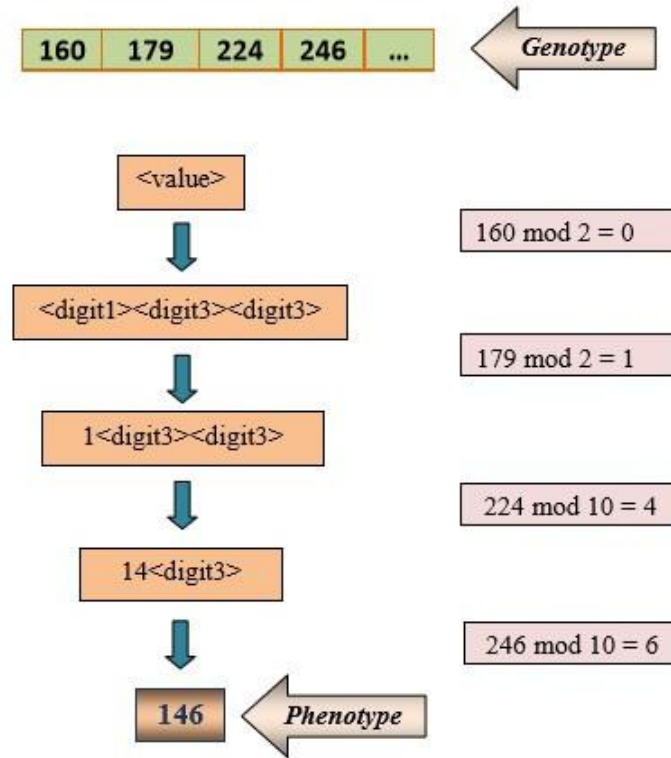


Fig. 4. Genotype-to-phenotype mapping process

B. Parameters Setting

The parameters of CGFWA are set as the following: number of fireworks

(NP) = 10, dimension (D), i.e., number of codons = $4K$, maximum number of explosion sparks for each firework = 40, boundary constraints on number of explosion sparks for each firework = [2, 32], magnitude of explosion = 255, number of Gaussian sparks = 10.

The parameters of CGS are set as the following: population size = 50,

(D) = $4K$, $V_{max} = 127.5$, $w_{min} = 0.4$, $w_{max} = 0.9$ $c_1 = c_2 = 1.49445$.

All the methods are allowed to run for maximum 5000 function evaluations (FES).

C. Termination Criteria

The termination criteria of all the methods are set as the following:

- There is no improvement for successive 20 iterations, or
- They complete the maximum number of FES .

IV. RESULT AND DISCUSSION

The CGFWA method is used for lesion detection to segment 25 breast DCE-MR images with cluster number $K = 3$. Comparative studies are performed with CGS and K-mean algorithms. The experiment is run for 51 independent runs for each image for each clustering techniques. The performance of the clustering methods is measured and validated using the familiar cluster validity index known as DB -index.

The Mean and standard deviations of DB -index over 51 separate runs are shown in Table 2. It has been observed from Table 2 that the lowest mean DB -index values are achieved by the proposed CGFWA for all the MR images. These quantitative results indicate that CGFWA performs better than the CGS and K-means algorithm.



To test the statistical significance i.e., validation of the quantitative results in Table 2, Wilcoxon Signed Ranks Test analysis [13] has been done and the statistics are shown in Table 3. It has been observed from Table 3. that CGFWA statistically outperforms GS and K-means with a significance level ($\alpha = 0.01$).

The qualitative results (i.e., visual) obtained from different methods for DCE- MRI slice # 5 (see Figure 5.) in dataset are given in Figure 6, 7 & 8. These resultant images are generated from the best run of 51 independent runs of each method. The clustered images are given in Figure 6. Images with extracted lesions only are given in Figure 7. The spotted lesions in MR images are given in Figure 8. It is observed from Figure 6(c) that abnormal tissues, i.e., lesions are not well separated from normal tissues in the breast using the K-means algorithm. That's why the extracted lesions in Figure 7(c) includes a large number of normal or healthy tissues in breast results in poor lesion detection. If a very closed look is made in Figure 6(b) compared to Figure 5, then it can be seen that some lesions are not well separated from healthy tissues using CGS. Compared to Figure 6(b) & 6(c), Figure 6(a) demonstrates that lesions are well separated from healthy tissues using CGFWA. Lesion area is calculated in terms of the total number of pixels belong to lesion region in Figure 7(a), 7(b) &

7(c). The calculated lesion areas are 482, 446, and 7380 for CGFWA, CGS, and K-means algorithms respectively.

From the analysis of the experimental results, it is observed that CGFWA outperforms CGS and K-means algorithms. The CGFWA is more efficient and effective than others in searching for the optimal cluster center of the MR image data results in better segmentation and detection of breast lesions in DCE-MRI.

The experiments are conducted on a high-end desktop PC having Intel(R) Core(TM) i7-4770 3.40 GHz CPU, 8GB RAM, Windows 2007 64-bit operating system, and Matlab 2016b software. CGFWA takes a computational time cost average of 146.09 seconds, CGS takes an average of 62.20 seconds and K-means takes average 0.11 seconds for lesion detection in breast DCE-MRI. The reason behind the high computational cost of CGFWA is the crowding distance-based selection mechanism which is computationally expensive. Other recent variants of FWA with a better selection strategy can be used as a search engine in GFWA to overcome this.

After the analysis of both quantitative and qualitative results, it is concluded that the devised CGFWA-based detection method outperforms both CGS and K-means algorithms.

Table 2 Mean and standard deviation (in parenthesis) of DB-index over 51 independent runs.

MRI#	CGFWA	CGS	K-means
1	0.0859(0.0009)	0.0868(0.0010)	0.1446(0.0001)
2	0.0901(0.0010)	0.0910(0.0010)	0.1479(0.0005)
3	0.0918(0.0007)	0.0927(0.0011)	0.1488(0.0011)
4	0.0900(0.0007)	0.0909(0.0010)	0.1517(0.0000)
5	0.0875(0.0003)	0.0880(0.0005)	0.1486(0.0000)
6	0.0876(0.0005)	0.0885(0.0010)	0.1425(0.0000)
7	0.0877(0.0005)	0.0882(0.0009)	0.1446(0.00001)
8	0.0877(0.0008)	0.0883(0.0008)	0.1470(0.0000)
9	0.0876(0.0004)	0.0883(0.0009)	0.1435(0.0002)
10	0.0876(0.0003)	0.0884(0.0011)	0.1381(0.0000)
11	0.0878(0.0010)	2.4234(0.0016)	0.1432(0.0004)
12	0.0875(0.0010)	2.0484(0.0011)	0.1331(1.90E-06)
13	0.0857(0.0007)	2.1074(0.0011)	0.1324(8.13E-17)
14	0.0833(0.0008)	1.6428(0.0016)	0.1259(5.61E-17)
15	0.0944(0.0015)	1.0931(0.0017)	0.1201(7.01E-17)
16	0.0911(0.0009)	1.5627(0.0014)	0.1139(8.41E-17)
17	0.0935(0.0012)	1.0845(0.0012)	0.1205(1.54E-16)
18	0.0941(0.0013)	1.2479(0.0013)	0.1204(4.83E-17)
19	0.0922(0.0018)	1.6923(0.0013)	0.1307(0.0002)
20	0.0899(0.0008)	1.2105(0.0013)	0.1787(0.01270)
21	0.0865(0.0010)	1.3431(0.0017)	0.1720(0.0147)
22	0.0918(0.0016)	1.0211(0.0015)	0.1885(0.0002)
23	0.0858(0.0015)	1.0845(0.0016)	0.1862(0.0121)
24	0.0867(0.0017)	1.2691(0.0013)	0.1808(0.0147)
25	0.0903(0.0012)	1.0693(0.0014)	0.1899(0.0133)



Table 3 Wilcoxon Signed Ranks Test Statistics on mean *DB-index* over 51 independent runs. R^+ : sum of positive ranks, R^- : sum of negative ranks.

Sl. No.	Comparison	R^+	R^-	Z	P(2-tailed)
1	CGFWA vs. CGS	325	0	-4.372	0.000012 < 0.01
2	CGFWA vs. K-means	325	0	-4.372	0.000012 < 0.01

V. CONCLUSION

In this paper, the GFWA-based clustering technique (i.e., CGFWA) is proposed to segment the breast DCE-MRI for lesion detection. GFWA is applied to automatically generate computer programs in any voluntary language. Here, GFWA is used to generate the cluster centers for MR image clustering. At the outset, MR images denoised and intensity inhomogeneities are corrected in the preprocessing step. The preprocessed MR images are segmented using CGFWA. Finally, the lesions are extracted from the segmented images. The experimental results (i.e., both quantitative and qualitative) of the proposed technique are compared with that of GS-based clustering and K-means clustering techniques and the

proposed method outperforms other methods. In this work, gray-level features are used in clustering. The wavelet-based features will be used in clustering techniques in the future works. The future work of this paper also points to the characteristics of breast lesions detected in DCE-MR image. In the proposed method, the cluster number is given explicitly by the user. An automatic clustering technique can be developed to automatically select the number of clusters in the image data. The proposed method takes higher computational time due to the time consuming crowding- based selection mechanism in FWA. The improved FWA with a faster selection mechanism will be used in the proposed method to make it more computationally efficient in the future.

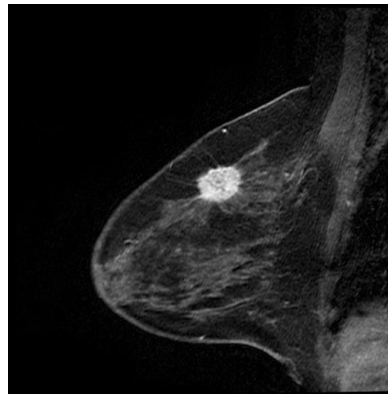


Fig. 5. DCE-MRI Slice #5

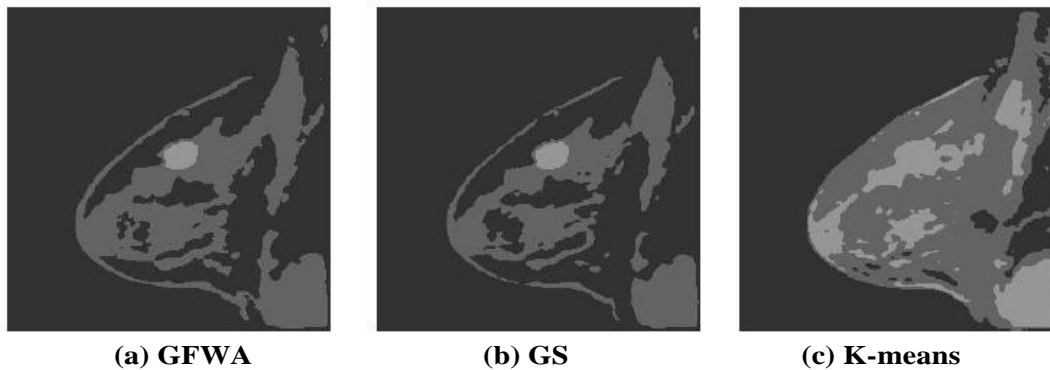


Fig. 6. Clustered images.

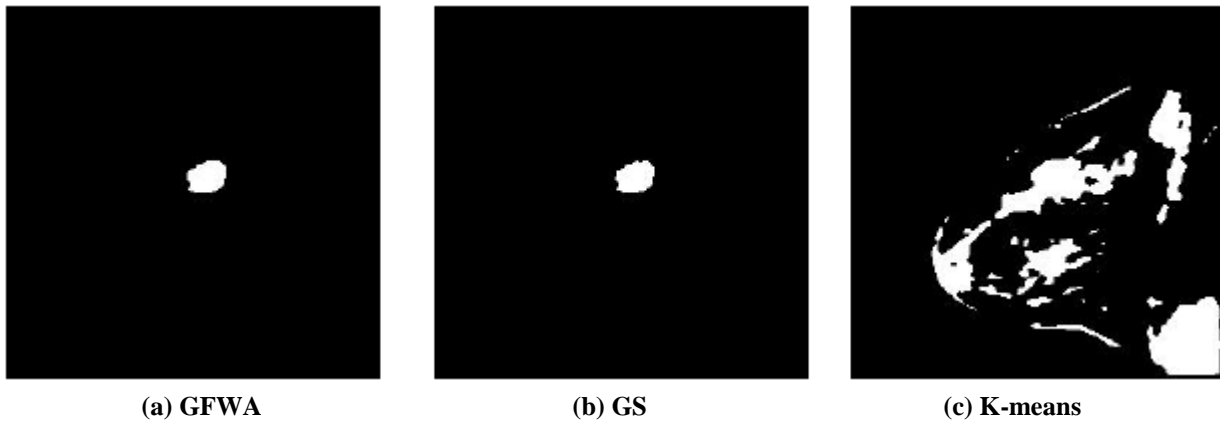


Fig. 7. Extracted breast lesions.

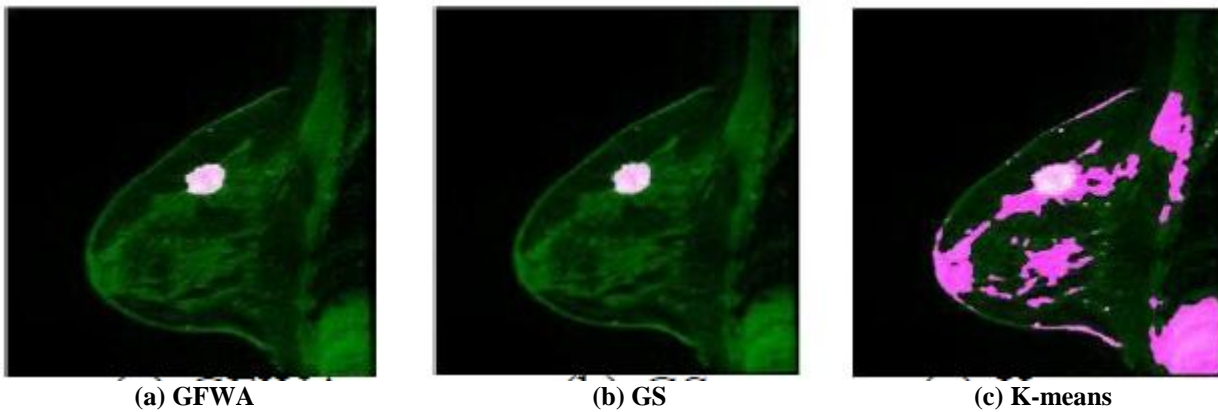


Fig. 8. Locations of lesions in MR images.

ACKNOWLEDGMENT

The authors are grateful to Dr. Tapas Si, of the Department of Computer Science and Engineering, Bankura Unnayani Institute of Engineering, Bankura, India, for valuable comments and help throughout the preparation of this paper.

REFERENCES

1. Agner, S.C., Soman, S., Libfeld, E., McDonald, M., Thomas, K., Englander, S., Rosen, M.A., Chin, D., Noshier, J., Madabhushi, A.: Textural kinetics: A novel dynamic contrast-enhanced (dce)-mri feature for breast lesion classification. *Journal of Digital Imaging* **24**, 446–63 (2011)
2. Arjmand, A., Meshgini, S., Afrouzian, R., Farzamnia, A.: Breast tumor segmentation using k-means clustering and cuckoo search optimization. *IEEE* (2019)
3. Azmi, R., Norozi, N.: A new markov random field segmentation method for breast lesion segmentation in mr images. *Journal of Medical Signals Sensors* **1**, 156–164 (2011)
4. Balafar, M., Ramli, A., Mashohor, S.: A new method for mr grayscale inhomogeneity correction. *Artif. Intell. Rev.* **34**, 195–204 (2010)
5. Bohare, M., Cheeran, A., Sarode, V.: Analysis of breast mri images using wavelets for detection of cancer. *IJCA Special Issue on Electronics, Information and Communication Engineering* **4**, 1–3 (2011)
6. Boukerroui, D., Basset, O., Guerin, N., Baskurt, A.: Multiresolution texture based adaptive clustering algorithm for breast lesion segmentation. *European Journal of Ultrasound* **8**, 135–144 (1998)
7. Bray, F., Ren, J.S., Masuyer, E., Ferlay, J.: Global estimates of cancer prevalence for 27 sites in the adult population in 2008. *Int J Cancer* **132**(5), 1133–45 (2013). DOI 10.1002/ijc.27711
8. Chang, Y.C., Huang, Y.H., Huang, C.S., Chang, P.K., Chen, J.H., Chang, R.F.: Classification of breast mass lesions using model-based analysis of the characteristic kinetic curve derived from fuzzy c-means clustering. *Magnetic Resonance Imaging* **30**(3), 312–322 (2012)
9. Chen, W., Giger, M.L., Bick, U.: A fuzzy c-means (fcm)-based approach for computerized segmentation of breast lesions in dynamic contrast-enhanced mr images. *European Journal of Ultrasound* **1**, 63–72 (2006)
10. Clark, K., Vendt, B., Smith, K., Freymann, J., Kirby, J., Koppel, P., Moore, S., Phillips, S., Maffitt, D., Pringle, M., Tarbox, L., Prior, F.: The cancer imaging archive (tcia): Maintaining and operating a public information repository
11. Cui, Y., Tan, Y., Zhao, B., Liberman, L., Parbhu, R., Kaplan, J., Theodoulou, M., Hudis, C., Schwartz, L.: Malignant lesion segmentation in contrast-enhanced breast mr images based on the marker-controlled watershed. *Medical physics* **36**, 4359–69 (2009)
12. Davies, D., Bouldin, D.: A cluster separation measure. *IEEE Trans. Pattern Anal. Mach. Intell.* **1**(2), 224–227 (1979)

13. Derrac, J., García, S., Molina, D., Herrera, F.: A practical tutorial on the use of nonparametric statistical tests as a methodology for comparing evolutionary and swarm intelligence algorithms. *Swarm and Evolutionary Computation* **1**, 3–18 (2011)
14. Ferlay, J., Soerjomataram, I., Ervik, M.: Globocan 2012 v1.0, cancer incidence and mortality worldwide: Iarc cancerbase. 11. GLOBOCAN (2013)
15. Ferlay, J., Soerjomataram, I., Ervik, M., Dikshit, R., Eser, S., Mathers, C., Rebelo, M., Parkin, D., Forman, D., Bray, F.: Globocan 2012 v1.0, cancer incidence and mortality worldwide: Iarc cancer base. no. 11 [internet]. In: F. Lyon (ed.) International Agency for Research on Cancer
16. Hamy, V., Dikaos, N., Punwani, S., Melbourne, A., Latifoltojar, A., Makanyanga, J., Chouhan, M., Helbren, E., Menys, A., Taylor, S., Atkinson, D.: Respiratory motion correction in dynamic mri using robust data decomposition registration - application to dce-mri. *Medical Image Analysis* **18**, 301–313 (2014)
17. Hauth, E., Stockamp, C., Maderwald, S., Mühler, A., Kimmig, R., Jaeger, H., Barkhausen, J., Forsting, M.: Evaluation of the three-time-point method for diagnosis of breast lesions in contrast-enhanced mr mammography. *Clinic Imaging* **30**, 160–165 (2006)
18. Jayender, J., Gombos, E., Chikarmane, S., Dabydeen, D., Jolesz, F., Vosburgh, K.: Statistical learning algorithm for in situ and invasive breast carcinoma segmentation. *Computerized Medical Imaging and Graphics* **37**, 281–292 (2013)
19. Khalvati, F., Ortiz, C.G., Balasingham, S., Martel, A.L.: Automated segmentation of breast in 3d mr images using a robust atlas. *IEEE Transactions on medical imaging* **34**, 116–125 (2015)
20. Lingle, W., Erickson, B.J., Zuley, M.L., Jarosz, R., Bonaccio, E., Filippini, J., N., G.: Radiology data from the cancer genome atlas breast invasive carcinoma collection [tcga-brca] (2007)
21. MacQueen, J.: Some methods for classification and analysis of multivariate observations. p. 281–297. University of California Press (1967)
22. McClymont, D., Mehnert, A., Trakic, A., Kennedy, D., Crozier, S.: Fully automatic lesion segmentation in breast mri using mean-shift and graph-cuts on a region adjacency graph. *J. Magn. Reson. Imaging* **39**, 795–804 (2014)
23. Milenković, J., Hertl, K., Košir, A., Žbert, J., Tasić, J.: Characterization of spatiotemporal changes for the classification of dynamic contrast-enhanced magnetic-resonance breast lesions. *Artificial Intelligence in Medicine* **58**(2), 101–114 (2013)
24. Mlejnek, M., Ermes, P., Vilanova, A., Rijt, R., Bosch, H., Gerritsen, F., Gröller, E.: Application-oriented extensions of profile flags (2006)
25. Mohan, J., Krishnavenib, V., Guo, Y.: A survey on the magnetic resonance image denoising methods. *Biomedical Signal Processing and Control* **9**, 56–69 (2014)
26. Nie, K., Chen, J., Yu, H., Chu, Y., Nalcioglu, O., Su, M.: Quantitative analysis of lesion morphology and texture features for diagnostic prediction in breast mri. *Acad. Radiol.* **15**, 1513–1525 (2008)
27. Perona, P., Malik, J.: Scale-space and edge detection using anisotropic diffusion. *IEEE Trans. Pattern Anal. Mach. Intell.* **12**(7), 629–639 (1990)
28. Piantadosi, G., Marrone, S., Galli, A., Sansone, M., Sansone, C.: Dce-mri breast lesions segmentation with a 3tp u-net deep convolutional neural network. *IEEE (2019)*
29. Shetty, M.: Breast Cancer Screening and Diagnosis - A Synopsis. Springer Science + Business Media, New York (2015)
30. Si, T.: Grammatical evolution using fireworks algorithm. In: M. Pant, K. Deep, J. Bansal, A. Nagar, K. Das (eds.) Proceedings of Fifth International Conference on Soft Computing for Problem Solving. Advances in Intelligent Systems and Computing, vol. 436. Singapore(2016)
31. Si, T., De, A., Bhattacharjee, A.: Brain mri segmentation for tumor detection using grammatical swarm based clustering algorithm. In: Proc. of IEEE International Conference on Circuits, Power and Computing Technologies (ICCPCT-2014), vol. 436. Nagercoil, India (2014)
32. Si, T., De, A., Bhattacharjee, A.: Grammatical swarm based segmentation methodology for lesion segmentation in brain mri. *International Journal of Computer Applications* **121**(4), 1–8 (2015)
33. Sim, K., Chia, F., Nia, M., Tso, C., Chong, A., Abbas, S., Chong, S.: Breast cancer detection from mr images through an auto-probing discrete fourier transform system. *Computers in Biology and Medicine* **49**, 46–59 (2014)
34. Tan, Y., Zhu, Y.: Fireworks algorithm for optimization. In: Y. Tan, Y. ShiKay, C. Tan (eds.) ICSI 2010, Part I, LNCS, vol. 6145, p. 355–364. Springer, Heidelberg (2010)
35. Tuncay, A.H., Akduman, I.: Realistic microwave breast models through r_l -weighted 3-d mri data. *IEEE Transactions on Biomedical Engineering* **62**(796305), 688–698 (2015)
36. Wang, Y., Morrell, G., Heibrun, M., Payne, A., Parker, D.: 3d multi-parametric breast mri segmentation using hierarchical support vector machine with coil sensitivity correction. *Acad. Radiol.* **20**, 137–147 (2013)
37. Wei, C.H., Li, Y., Huang, P., Gwo, C.Y., Harms, S.: Estimation of breast density: An adaptive moment preserving method for segmentation of fibroglandular tissue in breast magnetic resonance images. *European Journal of Radiology* **81**(4), e618–e624 (2012)
38. WHO <https://www.who.int/cancer/prevention/diagnosis-screening/breast-cancer/en/>. Accessed online: 05/12/2019
39. Wu, Q., Salganicoff, M., Krishnan, A., Fussell, D.S., Markey, M.K.: Interactive lesion segmentation on dynamic contrast enhanced breast mr using a markov model. *Proc. SPIE* (6144) (2006)
40. Yao, J., Chen, J., Chow, C.: Breast tumor analysis in dynamic contrast enhanced mri using texture features and wavelet transform. *IEEE Journal of selected topics in signal processing* **3**, 94–100 (2009)

AUTHORS PROFILE



Dipak Kumar Patra, holds B.Sc and M.Sc in Computer Science from Vidyasagar University Midnapore, W.B., India, and M.Tech in Computer Science and Engineering from Maulana Abul Kalam Azad University (formerly West Bengal University of Technology). He is currently State Aided College Teacher in the department of Computer Science & Application in Hijli College, Kharagpur, West Bengal, India. Presently he is a research scholar in Research Centre of Natural and Applied Sciences (Department of Computer Science), Raja Narendralal Khan Women's College (Autonomous), Midnapore-721102, West Bengal, India, His research interests include swarm intelligence and medical image processing.



Dr. Sukumar Mondal, holds B.Sc, M.Sc and Ph.D. in Mathematics from Vidyasagar University, Midnapore, W.B., India. He is currently an associate professor in the department of Mathematics in Raja Narendralal Khan Women's College, Midnapore, West Bengal, India. He publishes 28 papers in the reputed international journals/conferences. His research interests include Graph Theory, Fuzzy Graph Theory, swarm intelligence and medical image processing.



He is the recipient of Scientist of the year 2013 (NESA, New Delhi).
He has completed 4 Research Projects and produces 3 Ph. D. students.



Dr. Prakash Mukherjee, obtained Ph.D. degree in Pure Mathematics from University of Calcutta, Kolkata, West Bengal, India. He is currently a state aided college teacher in the department of Mathematics, Hijli College, Kharagpur, Midnapore, West Bengal, India. He has published 14 research papers in the International Journals. His area of interests is General Topology, Fuzzy Topology, image processing and Graph Theory.